

Barium Titanate: An emerging ferroelectric material for efficient electro-optic modulation

M Ifaz Ahmad Isti ^{*a}, Xiaofeng Zhu^a, Marco Tulio Moller de Freitas^a, Peng Yao^b, Shouyuan Shi^{a,b},
M. Jobayer Hossain^b, Timothy Creazzo^b, Dennis W. Prather^{a,b}

^aDepartment of Electrical and Computer Engineering, University of Delaware, Newark, DE 19716, USA

^bPhase Sensitive Innovations, Inc., Newark, DE 19713, USA

ABSTRACT

Barium Titanate (BTO) is a material having a robust electro-optic effect (due to a large Pockel's coefficient), high 2nd-order nonlinearity, low 3rd-order nonlinearity, ultra-low optical absorption with pure phase modulation, broad transmission spectrum and linear response to an applied field, which makes it an ideal candidate for developing Electro-Optic modulators (EOMs). Herein, we present a fabrication process development to realized low-loss monolithic waveguides on a thin-film BTO material platform. The study includes the material's suitability for low-loss waveguides in an optical simulation environment built on Lumerical Mode solver and the characterization of fabricated waveguides using atomic-force microscopy, scanning electron microscopy and optical back-scattering reflectometry.

Keywords: Electro-Optic modulators, optical backscattering, low-loss waveguides, waveguide fabrication, guided mode, BTO thin film, ferroelectric domain

1. INTRODUCTION

Miniaturization of photonic devices and their implementation into a photonic integrated platform is becoming an urgent capability when it comes to high-speed data transmission for long-haul fiber optic communications. For that, EOMs are the primary are the means to attain that. And these devices address a wide-range of applications in on-chip RF photonic devices, signal splitting, sensing, frequency comb generation, wavelength converters, transducers, and so more [1]. Lithium Niobate (LN) is another material that has gained high popularity in the recent past, in particular, when it comes to designing photonic platforms. However, the application of lithium niobite as a bulk material certainly limits its potential. As a result, fabrication process was developed to realize high-quality thin films of lithium niobite prepared from the "smart cut" process, which involves crystal ion slicing and wafer bonding. This led to the development of ultra-low loss miniaturized lithium niobite waveguides having relatively high index contrast, which ensures robust mode confinement. Such tight confinement of the optical mode reduces its overlap with sidewall roughness leading to lower optical losses, which in turn enable a more efficient electro-optic material. However, compared to LN, BTO is far superior when it comes to the application of these materials in making EO modulators, as the electro-optic coefficient of BTO is more than 40 times that of LN.

The electro-optic effect of the material is responsible for the interaction of the RF and the optical field, which makes the material suitable for its application in optical modulation, frequency shifting, and nonlinear optics. The crystal orientation of LN and BTO beholds 3-fold rotation symmetry about the z-axis, commonly referred to as the 'c-axis.' Their non-centrosymmetric crystal structure gives it a high 2nd - order non-linear coefficient ($d_{33} = -27\text{pm/V}$ for LN and $d_{33} = 6.8\text{pm/V}$ for BTO) [2 – 3]. The high Pockel's coefficient of LN ($r_{33} = -31\text{pm/V}$) gives the material good EO properties. Alternatively, BTO has a Pockel's coefficient as high as $r_{33} = 105\text{pm/V}$ and $r_{42} = 1300\text{pm/V}$, which makes the material an exceptional candidate for EOMs [4].

Coming to the implementation of optical modulators, the most effective configurations are Mach-Zehnder Interferometer, Michelson Interferometer, resonator structures, (micro-ring, micro-disk, photonic crystal), plasmonic absorber-based Intensity modulators, Z-cut modulators, and plasma dispersion effect based PN-junction/MOS driven Silicon EO modulators [5 – 8]. A common scenario in all these types of modulators is altering the effective refractive index of the guided light with the application of an external field to control and manipulate light within the waveguide that follows the

*ifazisti@udel.edu; phone 1 412 579-3291

applied DC/RF bias. The primary goal of this research is to develop high-efficiency EOMs on a BTO material platform, which can make them noteworthy in terms of key features like Half-Wave Voltage (V_π), EO bandwidth, insertion loss, and extinction ratio with respect to modulators based on other material platforms. When it comes to the ‘optical’ part of the device, guiding of light can be achieved with strip-loaded waveguides and ridge-etched waveguides [9 – 10]. The modal confinement is higher in the later, which can give rise to a better EO effect, but this may increase the propagation losses as the mode interacts more with the etched sidewall roughness. Another challenge is miniaturization of the device length, as mentioned earlier, in order to realize a ‘folded’ MZI with a 180° bend, which can significantly shorten the overall device length. In this case, poling can be done in the folded region to invert the ferroelectric domain, or one can utilize waveguide crossings. One can also use interdigitated T-rails as CPW electrodes or segmented electrodes to realize a high-speed, high bandwidth, lower insertion loss, and lower V_π device [1]. Herein, we present monolithic waveguides on BTO thin-film material platform that has low propagation losses. Atomic-Force Microscopy (AFM) and Scanning Electron Microscopy reveal the qualitative condition of the waveguides and optical back-scattering reflectometry reveals the propagation losses for their quantitative evaluation.

2. THEORETICAL CONSIDERATIONS AND MATERIAL PROPERTIES

The application of an electric field externally can cause alterations to the shape of the index ellipsoid, which is given by [3]:

$$\left[\frac{1}{n_x^2} + \Delta\left(\frac{1}{n^2}\right)_1 \right] x^2 + \left[\frac{1}{n_y^2} + \Delta\left(\frac{1}{n^2}\right)_2 \right] y^2 + \left[\frac{1}{n_z^2} + \Delta\left(\frac{1}{n^2}\right)_3 \right] z^2 + 2\Delta\left(\frac{1}{n^2}\right)_4 yz + 2\Delta\left(\frac{1}{n^2}\right)_5 xz + 2\Delta\left(\frac{1}{n^2}\right)_6 xy = 1. \quad (1)$$

$$\text{Here, } \Delta\left(\frac{1}{n^2}\right)_i = \sum_{j=1}^3 r_{ij} E_j, \text{ where } \Delta n = -\frac{1}{2} n_e^3 r_{33} E_z. \quad (2)$$

The impermeability tensor $\Delta\left(\frac{1}{n^2}\right)_i$ is a function of the applied field strength and r_{ij} , the propensity vector is better described as the EO coefficient. Equation 2 delineates the refractive index (RI) alterations in the z -orientation with the application of a z -oriented field E_z . This equation describes the linear relation between the RI alterations and the applied field, widely recognized as the Pockels effect.

Table 1. Comparison of different EO materials [3].

Material	RI	ϵ_r	$r(\text{pm/V})$
LiNbO ₃	2.29	84	30.9
BaTiO ₃	2.37	4500	730
LiTaO ₃	2.23	51	31
PbTaO ₃	2.67	115	5.9
KNBO ₃	2.23	160	64
BiFeO ₃	3	30-50	12

LN and BTO materials cover a broad transparency window (400nm-5 μ m wavelength), which makes it suitable for its application in quantum computation, frequency metrology, and LIDAR applications. Transparency at 1550nm (telecommunication regime) makes the LN and BTO useful for telecommunications applications.

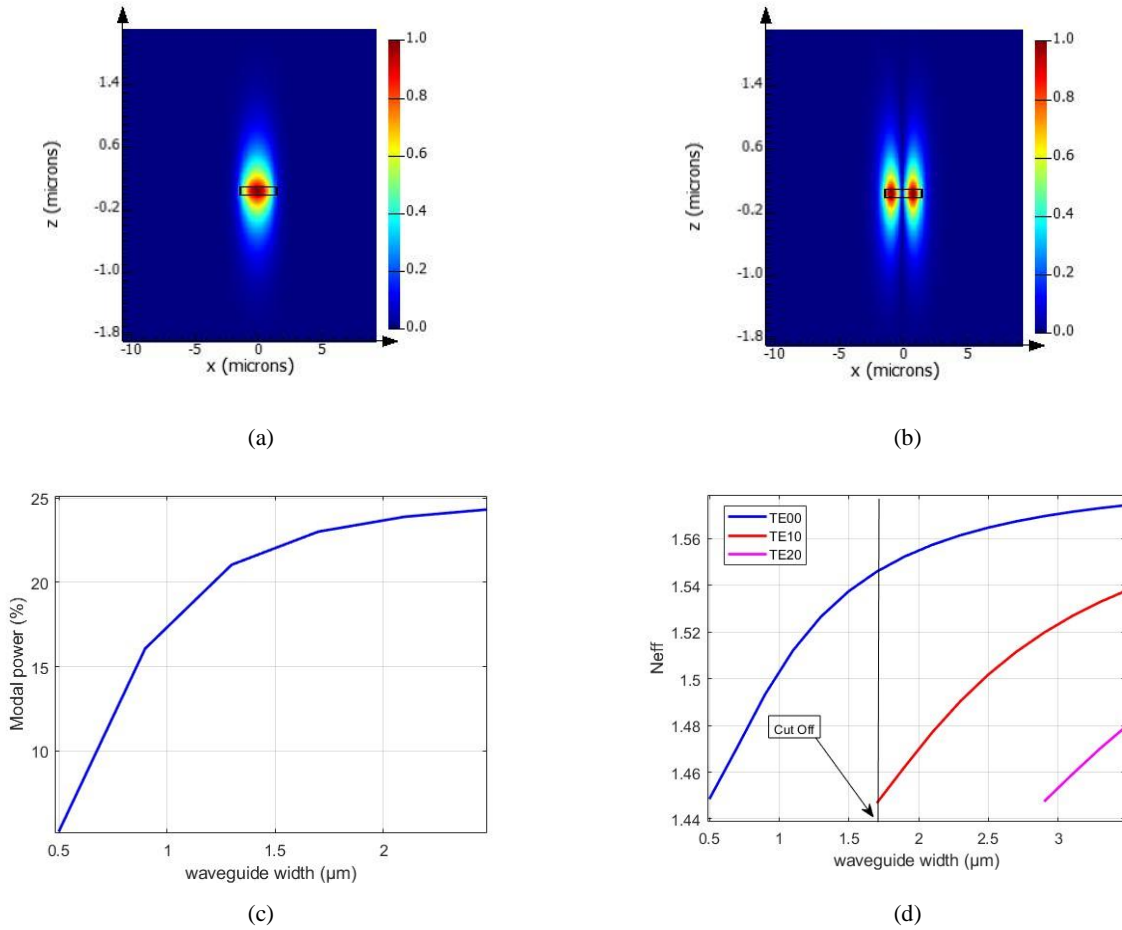


Figure 1. Guided modes confined in the waveguides (a) Fundamental TE mode (b) 2nd order TE mode (c) Modal power confinement variations along the waveguide width with a thickness of 150nm, and (d) effective indices of different TE modes as a function of waveguide width

3. DESIGN SCHEMES AND FABRICATION

The efficiency of the EO modulation partly depends on the optical part of the device, specifically how well the guided mode is confined in the waveguide with lower propagation losses. Lumerical mode simulation reveals the mode confinement within the fully etched BTO waveguide with a thickness of 150nm portrayed in Figure 1. A waveguide width of 1.7 μ m is the cutoff width for the single mode condition above which the waveguide becomes multimode. Due to the sputter growth limitations to keep the BTO film single crystalline, a thickness of 150nm is chosen. As evident from Figure 1(c), the modal power confinement increases with increased waveguide width which is more desired.

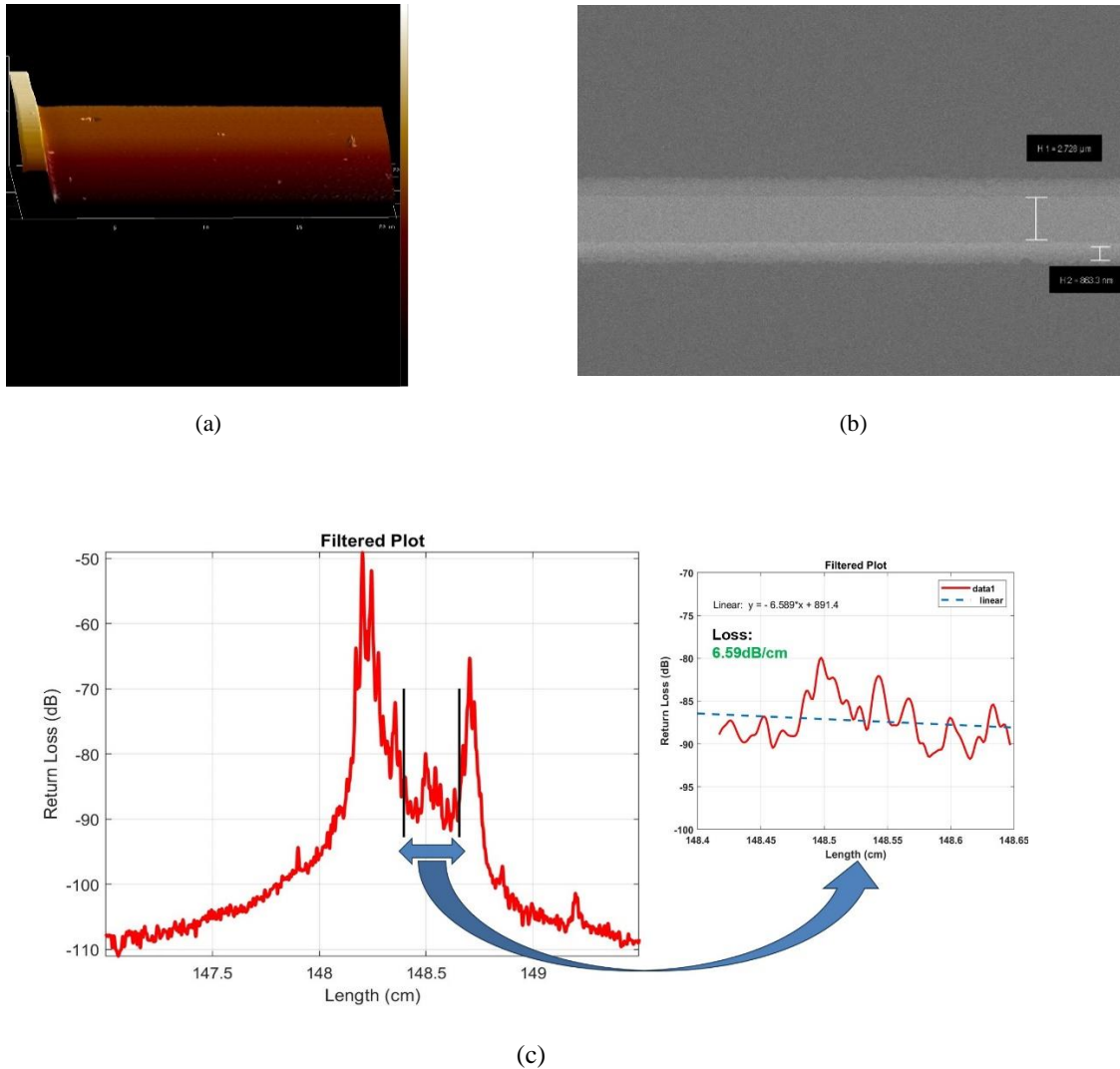


Figure 2. (a) AFM reveals smooth surface and low sidewall roughness at lower RF bias power (b) SEM portrays the smooth sidewall roughness, and (c) OBR reveals waveguide propagation losses of 6.6dB/cm

BTO films are grown using a sputter deposition, which is compatible with the state-of-the-art industrial fabrication processes. The ferroelectric domains are oriented in four different directions, which is responsible to some extent for waveguide propagation losses. Spin-coating the film with negative resist, Electron Beam Lithography (EBL) is used to pattern the waveguides. Ion Beam Milling (IBM) with different high and low bias power etches the waveguide where the surface condition is profiled with AFM, shown in Figure 2 after removing the resist. A higher bias power produces rougher surfaces and sidewalls a lower bias. Smooth sidewalls and surfaces of the waveguides are desired for lower propagation losses. The resist is removed with acetone and NMP immersed in 80° water-bath. Optical back-scattering reflectometry is applied to extract the waveguide losses. A 1550nm laser source launches light into the waveguide over a polarization-maintaining optical fiber that passes through the waveguide and reflects light at all points that later develops the reflection peak profiles, illustrated in Figure 2(c). The two Gaussian peaks are the reflection peaks at the extreme ends of the waveguide. A linear fit of all the data within the reflection peaks produces a straight line. The absolute value of the slope is the waveguide propagation loss.

4. CONCLUSION

In summary, we have developed a fabrication process to realize low-loss monolithic Barium Titanate waveguides that can be directly used to couple the optical and RF fields by inserting electrodes. Our atomic force microscopy and scanning electron microscopy reveal the smooth surface and sidewall roughness of the waveguides. The propagation losses observed within the waveguides are mostly due to the random ferroelectric domains within the crystal which scatter light in different directions and also the crystal growth quality.

ACKNOWLEDGEMENTS

The authors would like to acknowledge the support of Dr. Deborah Van Vetchen at the Office of Naval Research as well as device teams at the University of Delaware and Phase Sensitive Innovations.

REFERENCES

- [1] Chen, Guanyu, Yuan Gao, Hong-Lin Lin, and Aaron J. Danner. "Compact and Efficient Thin-Film Lithium Niobate Modulators." *Advanced Photonics Research* 4, no. 12 (2023): 2300229
- [2] Ahmed, Abu Naim R., Sean Nelan, Shouyuan Shi, Peng Yao, Andrew Mercante, and Dennis W. Prather. "Subvolt electro-optical modulator on thin-film lithium niobate and silicon nitride hybrid platform." *Optics letters* 45, no. 5 (2020): 1112-1115
- [3] Karvounis, Artemios, Flavia Timpu, Viola V. Vogler-Neuling, Romolo Savo, and Rachel Grange. "Barium titanate nanostructures and thin films for photonics." *Advanced Optical Materials* 8, no. 24 (2020): 2001249
- [4] Kim, Inhwan, Therese Paoletta, and Alexander A. Demkov. "Nature of electro-optic response in tetragonal BaTiO₃." *Physical Review B* 108, no. 11 (2023): 115201.
- [5] Chen, Guanyu, Nanxi Li, Jun Da Ng, Hong-Lin Lin, Yanyan Zhou, Yuan Hsing Fu, Lennon Yao Ting Lee, Yu Yu, Ai-Qun Liu, and Aaron J. Danner. "Advances in lithium niobate photonics: development status and perspectives." *Advanced Photonics* 4, no. 3 (2022): 034003-034003.
- [6] Desiatov, Boris, Amirhassan Shams-Ansari, Mian Zhang, Cheng Wang, and Marko Lončar. "Ultra-low-loss integrated visible photonics using thin-film lithium niobate." *Optica* 6, no. 3 (2019): 380-384.
- [7] Renaud, Dylan, Daniel Rimoli Assumpcao, Graham Joe, Amirhassan Shams-Ansari, Di Zhu, Yaowen Hu, Neil Sinclair, and Marko Loncar. "Sub-1 Volt and high-bandwidth visible to near-infrared electro-optic modulators." *Nature Communications* 14, no. 1 (2023): 1496.
- [8] Sinatkas, Georgios, Thomas Christopoulos, Odysseas Tsilipakos, and Emmanouil E. Kriezis. "Electro-optic modulation in integrated photonics." *Journal of Applied Physics* 130, no. 1 (2021).
- [9] Xiong, Chi, Wolfram HP Pernice, Joseph H. Ngai, James W. Reiner, Divine Kumah, Frederick J. Walker, Charles H. Ahn, and Hong X. Tang. "Active silicon integrated nanophotonics: ferroelectric BaTiO₃ devices." *Nano letters* 14, no. 3 (2014): 1419-1425.
- [10] Posadas, Agham B., Vincent E. Stenger, John D. DeFouw, Jamie H. Warner, and Alexander A. Demkov. "RF-sputtered Z-cut electro-optic barium titanate modulator on silicon photonic platform." *Journal of Applied Physics* 134, no. 7 (2023).